



Contents lists available at ScienceDirect

Acta Biomaterialia

journal homepage: [www.elsevier.com/locate/actabiomat](http://www.elsevier.com/locate/actabiomat)

## 5-Fluorouracil–lipid conjugate: Potential candidate for drug delivery through encapsulation in hydrophobic polyester-based nanoparticles

N. Ashwanikumar<sup>a</sup>, Nisha Asok Kumar<sup>b</sup>, S. Asha Nair<sup>b</sup>, G.S. Vinod Kumar<sup>a,\*</sup>

<sup>a</sup> Chemical Biology, Rajiv Gandhi Centre for Biotechnology, Poojappura, Thiruvananthapuram 695 014, Kerala, India

<sup>b</sup> Cancer Research Programme, Rajiv Gandhi Centre for Biotechnology, Poojappura, Thiruvananthapuram 695 014, Kerala, India

### ARTICLE INFO

#### Article history:

Received 11 March 2014

Received in revised form 23 July 2014

Accepted 30 July 2014

Available online xxx

#### Keywords:

Polyester  
5-Fluorouracil  
Palmitic acid  
Nanoparticles

### ABSTRACT

The encapsulation of 5-fluorouracil (5-FU) in hydrophobic polymeric materials is made feasible by a lipid-based prodrug approach. A lipid–5-FU conjugate of 5-FU with palmitic acid was synthesized in two-step process. A synthesized dipalmitoyl derivative (5-FUDIPAL) was characterized using Fourier transform infrared spectroscopy and <sup>1</sup>H-nuclear magnetic resonance. The 5-FUDIPAL was encapsulated in polyester-based polymers by the double emulsion–solvent evaporation method. The nanoparticles were characterized by scanning electron microscopy, transmission electron microscopy and dynamic light scattering. The thermal stability was assessed by differential scanning calorimetry data. In vitro release kinetics measurements of the drug from nanoparticles showed the controlled release pattern over a period of time. Cytotoxicity measurements by MTT assay confirmed that dipalmitoyl derivative in nano formulation successfully inhibited the cell growth. Thus the combined physical and biological evaluation of the different polyester-based nanoparticle containing the modified drug showed a facile approach to delivering 5-FU to the tumour site with enhanced efficacy.

© 2014 Acta Materialia Inc. Published by Elsevier Ltd. All rights reserved.

### 1. Introduction

Nanomaterials were able to contribute a new dimension to the field of controlled drug delivery systems (CDDS) with a novel generation of therapeutics with enhanced efficacy and diminished backlash [1]. Materialistic blending of drugs with polymers is normally accomplished by encapsulation of drugs in polymer nanoparticles, dendrimers micelles or hydrogels [2,3]. Polymeric nanoparticles with encapsulated drugs have been proved to be effective and extensively useful for therapeutic purposes [4]. The impact of encapsulation of small molecules inside the large polymeric matrix depends mainly on the nature of the small molecules, the hydrophilicity of the small molecules, the number of reactive functional groups and the stability of the molecules [5–7]. The extent of incorporation of the drug into the polymeric matrix depends mainly on the hydrophobicity of the drug and polymer. Usually, hydrophilic drugs such as 5-fluorouracil (5-FU) show lower encapsulation efficacy in polyester-based nanoparticles such as poly(lactide-co-glycolide) (PLGA), polylactic acid (PLA) and polycaprolactone (PCL) [8–10].

Polyesters such as PLGA, PLA and PCL are USFDA (United States Food and Drug Administration) approved materials for

drug-delivery systems. Several nanoformulations of these materials have been evaluated for various malignancies, such as colon cancer, breast cancer and ovarian cancer [11]. The biodegradable nature of these aliphatic polyesters is due to the facile hydrolysable ester backbone, which on degradation gives simple molecules such as carbon dioxide and water [12]. The inherent structure of these polymers constitutes the hydrophobic nature of these polymers, which limits their use in the encapsulation of hydrophilic molecules. Low encapsulation efficiency, fast diffusion of the drug from the polymeric matrix and the limited controlled release phenomenon observed in vitro are some of the flaws in the loading of hydrophilic entities inside these polymers [13].

5-FU is a major drug used in the treatment of colon cancer. Although it acts in several ways, it principally acts as a thymidylate synthase (TS) inhibitor resulting in the depletion of thymidine in nucleotide synthesis. TS catalyses the reductive methylation of deoxyuridine monophosphate to give deoxythymidine monophosphate (dTMP). Administration of 5-FU leads to a deficiency of dTMP, and the fast-dividing malignant cells undergo “thymineless cell death” [14]. The clinical use of 5-FU is normally accompanied by various side effects [15]. The treatment of 5-FU has several shortcomings, such as rapid drug catabolism and poor absorption owing to dihydropyrimidine dehydrogenase (DPD) enzyme [16], short biological half-life of the drug (10–20 min in blood plasma),

\* Corresponding author. Tel.: +91 471 2529526; fax: +91 471 2348096.

E-mail address: [gsvinod@rgcb.res.in](mailto:gsvinod@rgcb.res.in) (G.S. Vinod Kumar).

and poor and non-selective action against healthy cells of gastrointestinal tract and bone marrow [17].

Several attempts to minimize these side effects have been explored earlier. They include synthesis of 5-FU derivatives with low molecular weight [18], conjugation with other compounds and polymeric materials [19] and encapsulation in polymers [20]. The encapsulation of 5-FU in hydrophobic polymeric materials will be made feasible by a lipid-based prodrug approach. The synthesized prodrug can be encapsulated inside the polymeric nanoparticles using conventional methods such as the double emulsion/solvent evaporation technique. The metabolic pathways of fatty acids, facile cleavage of the ester bond of lipid–drug conjugate in *in vitro* conditions and a higher amount of prodrug loading inside the polymeric nanoparticle are some of the potential benefits of this type of approach [21].

In the present study, 5-FU is modified with a lipid, namely palmitic acid, to give a dipalmitoyl derivative, i.e. 5-FUDIPAL. The synthesized lipid–drug conjugate was characterized by Fourier transform infrared spectroscopy (FT-IR) and nuclear magnetic resonance (NMR) and the thermal stability of 5-FUDIPAL was measured by differential scanning calorimetry (DSC). Then the modified drug-encapsulated nanoparticles were prepared with polyesters such as PLGA, PCL and PLA. The size and morphology of the nanoparticles were characterized using transmission electron microscopy (TEM), scanning electron microscopy (SEM) and dynamic light scattering (DLS). The thermal behaviour of the nanoparticles was also monitored using DSC. The distribution of 5-FUDIPAL inside the nanoparticles was analysed by X-ray powder diffraction analysis (XRPD). *In vitro* drug release was assessed to study the drug release behaviour of the nanoparticles. Further, the biological evaluation in HCT-116 (colon cancer cell line) by MTT (3-[4,5-dimethylthiazol-2-yl]-2, 5-diphenyltetrazolium bromide) assay revealed the efficacy of 5-FUDIPAL in inducing cytotoxicity in both naïve and nano formulation.

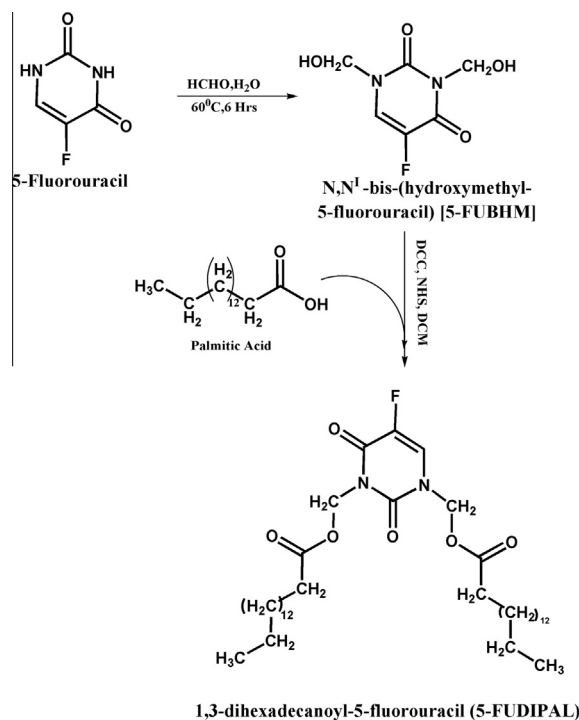
## 2. Materials and methods

### 2.1. Reagents

Palmitic acid, 5-FU, formaldehyde, MTT, *N,N*-dicyclohexylcarbodiimide (DCC), *N*-hydroxysuccinimide (NHS), PLA, PLGA, PCL and all other chemicals were purchased from Sigma-Aldrich (Steinheim, Germany). Fetal bovine serum (FBS) was purchased from Gibco (Life Technologies AG, Basel, Switzerland) and RPMI-1640 from Invitrogen. All organic solvents were of high-performance liquid chromatography (HPLC) grade.

### 2.2. Synthesis of 5-FUDIPAL

The synthetic pathway to the 5-FU–palmitic acid conjugate was performed according to Scheme 1. Briefly 5-FU (0.65 g, 10 mmol) and formaldehyde (1.34 g, 25 mmol) in aqueous solution were added to water (10 g) in a 100-ml round-bottom flask, which was immersed in a 60 °C oil bath [22,23]. The reaction was conducted under magnetic agitation for 6 h. The resultant solution was concentrated using a rotary evaporator and then dried in a vacuum oven at 60 °C for 48 h. The product was obtained according to Scheme 1 as *N,N*-1, 3-bis(hydroxymethyl-5-fluorouracil) abbreviated as 5-FUBHM (65 mol.%). The product was purified by column chromatography and analysed for the presence of traces of formaldehyde using the HPLC system (Waters-515, equipped with UV/Vis Detector- 2489 and Sun Fire™ (C18, 5 µm) column) as reported earlier [24]. Then, 5-FUBHM was subjected to palmitoylation. Palmitic acid (2.56 g, 10 mmol) was taken in a double-neck round-bottom flask, and DCC and NHS were taken in a molar ratio 1:2.5:2.5.



**Scheme 1.** Synthesis of 5-FUDIPAL. Schematic representation of 5-FUDIPAL synthesis by two-step process.

Distilled dichloromethane (DCM) was used as the solvent. The reaction mixture was agitated for 24 h at room temperature. The precipitated dicyclohexyl urea was separated by filtration. The activated 5-FUBHM (0.35 g, 5 mmol) was added to the reaction mixture and stirring continuously for 48 h. The entire process was carried out in dark conditions and an inert atmosphere. The product formed was precipitated using diethyl ether and purified by washing repeatedly with acetone to remove impurities.

### 2.3. Characterization of 5-FUDIPAL

#### 2.3.1. FT-IR spectra

The two steps of synthesis were characterized using FT-IR (Perkin Elmer, Spectrum 65-FTIR spectrometer). For each sample, eight scans were collected and averaged to reduce the signal to noise ratio. The spectral range was 4000–600 cm<sup>−1</sup>.

#### 2.3.2. <sup>1</sup>H-NMR

The NMR spectrum of the polymer was taken in a Bruker, 500 MHz spectrometer. D<sub>2</sub>O and CDCl<sub>3</sub> were used as the solvents for 5-FUBHM and 5-FUDIPAL, respectively.

### 2.4. Preparation of polyester nanoparticles loaded with 5-FUDIPAL

The double-emulsion solvent–evaporation technique (water-in-oil-in-water) was used to prepare the 5-FUDIPAL loaded polyester (i.e. PLGA, PLA, PCL) nanoparticles [25]. Briefly, 5 ml of a certain concentration of 5-FUDIPAL solution was emulsified in 10 ml of polyester–DCM solution under high-speed stirring (BO-1 magnetic stirrer, Shanghai Shiyuan Science and Equipment Co., Ltd., Shanghai, China). The resulting primary emulsion was added to an aqueous solution (50 ml) containing a given surfactant non-ionic Tween 80 (1% v/v) under stirring to form the double emulsion. The resultant solution was sonicated using Vibra-Cel™ Sonics; at 130 W and 20 kHz power supply for 3 min. DCM was eliminated by evaporation under reduced pressure with a rotary evaporator (IKA® RV 10 digital, Wilmington, NC, USA.). The resulting NP were

recovered by ultracentrifugation at 40,000 rpm (Optima™-100 K Ultracentrifuge, Beckman Coulter Inc, Brea, CA) at 4 °C for 1 h. The nanoparticle suspension was lyophilized (VirTis®, AdVantage, Warminster, PA) at a condenser temperature of –55 °C, using sucrose as the stabilizer (20% w/v) [26].

## 2.5. Determination of drug encapsulation efficiency

A known amount of the lyophilized 5-FUDIPAL loaded nanoparticles were dissolved in DCM and vortexed vigorously to get a clear solution and kept for 24 h. Then the solution was filtered through a 0.1 µm membrane filter (MILLEX® – VV, Syringe driven filter unit, Millipore, Ireland). Absorbance of the filtrate was taken as 266 nm using UV absorbance (Perkin Elmer, USA). The encapsulated 5-FUDIPAL content in the nanoparticles was determined by the ratio of actual encapsulating ratio (AER) to theoretical encapsulating ratio (TER), expressed in terms of amount of prodrug per weight of nanospheres. The encapsulation efficiency can be calculated by the equation:

$$\text{encapsulation efficiency (\%)} = \text{AER/TER} \times 100$$

$$\begin{aligned} (\text{AER} = \text{measured prodrug wt./measured nanoparticle wt.}; \text{TER} \\ = \text{initial prodrug wt./initial polymer(polyester) wt.}) \end{aligned}$$

## 2.6. Characterization of nanoparticles

### 2.6.1. Particle size analysis

The particle size of the 5-FUDIPAL nanoparticles was measured by the DLS method using a Delsa™ Nano particle size analyzer (Beckman Coulter, Inc.) instrument at ambient temperature. The samples were analyzed without prior filtration.

### 2.6.2. Zeta potential measurements

The surface charge of the 5-FUDIPAL encapsulated polyester nanoparticles was analysed by zeta potential measurements using a Zetasizer Nano ZS (Malvern Instruments, Malvern, UK) instrument at ambient temperature. The nanoparticle concentration was 0.1 mg ml<sup>–1</sup> in water and analysed without filtration.

### 2.6.3. TEM analysis

Morphological studies of the nanoparticles were characterized by TEM (JEOL 1011, Japan). The drug-loaded nanoparticle (0.5% w/v, 0.05% w/v) dissolved in Milli-Q® (Millipore Corporation, Billerica, MA) water was dropped on a copper-coated formavar microscopy grid. The grid was washed with 1 µl Milli-Q water. The sample on the grid surface was allowed to dry at room temperature in a desiccator containing calcium chloride, and measurements were taken. TEM pictures were taken using Digital Micrograph and Soft Imaging Viewer software.

### 2.6.4. SEM analysis

The surface morphology of the prepared polyester nanoparticles was characterized by SEM analysis, using EVO 18 Special Edition and a Carl Zeiss instrument. Prior to analysis, samples were sputter-coated with gold in order to make the surface conductive for 165 s.

### 2.6.5. DSC analysis

DSC was performed to analyse the state of 5-FUDIPAL dispersed inside the polymeric matrix. DSC thermograms were obtained using an automatic thermal analyser system (Pyres DSC 6000, Perkin-Elmer, USA). Samples were crimped in standard aluminium pans and heated from 20 to 310 °C at a rate of 10 °C min<sup>–1</sup> under constant purging of N<sub>2</sub> at 10 ml min<sup>–1</sup>. An empty pan, sealed in the same way as the sample, was used as a reference.

### 2.6.6. XRPD analysis

The distribution of lipid–drug conjugate inside polymeric nanoparticles and the amorphous nature of the nanoparticles was assessed by XRPD analysis. The X-ray diffraction patterns were obtained on a D8-Advance Bruker-AXS diffractometer using Cu K<sub>α</sub> irradiation. The experiments were performed at a scanning rate of 4° min<sup>–1</sup> in the 2θ range 5–40° in continuous mode.

## 2.7. In vitro drug release studies

The release of 5-FUDIPAL from different nanoparticulate systems was studied by performing in vitro drug release. The weighed amount of the four different nanoparticles containing 5-FUDIPAL (10 mg each) was dispersed in a solution of 50 ml freshly prepared phosphate buffered saline (PBS), pH 7.4, containing Tween®-80 (0.1%, w/v). The reaction mixture was incubated at 37 °C and subjected to continuous shaking at 90 rpm, using a rotary shaker. The controlled release pattern was observed for 900 min. At different time intervals, 1 ml of the reaction mixture was withdrawn. The amount of 5-FUDIPAL release was estimated using a UV–Visible Spectrophotometer (Perkin-Elmer, Lambda 25) at 266 nm.

## 2.8. Cell culture

Human colorectal carcinoma cell line (HCT 116) cells were purchased from American Type Culture Collection (Manassas, VA) and maintained in RPMI-1640 (Invitrogen, Carlsbad, CA) supplemented with 10% FBS and a 1% antibiotic–antimycotic cocktail (Life Technologies, AG, Basel, Switzerland) at 37 °C under a humidified atmosphere containing 5% carbon dioxide. Until reaching 70% confluence in tissue culture flasks, the cells were trypsinized with PBS solution containing 0.25% trypsin and 0.03% EDTA.

## 2.9. Cell cytotoxicity assay

An MTT reduction assay was performed to assess cell cytotoxicity. Cells were seeded into a 96-well plate (5 × 10<sup>3</sup> cells well<sup>–1</sup>) and incubated under standard growth conditions for 24 h at 60–70% confluence. Cells were then treated with formulations of 5-FU (1–100 µM) and 5-FUDIPAL (1–100 µM) for 24, 48 and 72 h. After the respective hours of drug treatment, the cells were again incubated for 4 h with 10% v/v MTT (5 mg ml<sup>–1</sup> dissolved in PBS pH 7.4). The medium was then removed completely, and the formazan crystals so formed were dissolved in 100 µl isopropyl alcohol. Absorbance was measured at 570 nm using a Biorad plate reader Model 680. The same experiment was repeated with different polyester-based nanoparticulate systems of 5-FUDIPAL.

The percentage inhibition was calculated using the formula (avg. OD of control – avg. OD of test)/avg. OD of control × 100

## 2.10. Statistics

All the measurements were done in triplicate, and the results expressed as arithmetic mean ± standard error of the mean. Statistical analysis of the data was assessed by Student's *t*-test. A value of significance *p* < 0.05 was considered significant (*n* = 3).

## 3. Results

### 3.1. Preparation of 5-FUDIPAL

The 5-FU reacts with aqueous formaldehyde (in stoichiometric excess) to give 5-FUBHM in quantitative yield. The excess amount of aq. formaldehyde ensures the complete conversion of 5-FU to

5-FUBHM with 69% yield, along with other compounds such as mono hydroxymethyl substituted 5-FU. The chromatographic separation of 5-FUBHM with high purity (without the traces of formaldehyde, as shown in the HPLC curve) was then subjected to the second step, as depicted in Scheme 1. The conjugation of palmitic acid with DCC/NHS chemistry was also achieved successfully with 82% yield. The 5-FUDIPAL formed was soluble in non-polar solvents such as dichloromethane and chloroform, whereas it was insoluble in water. The conjugation of two lipid tails would be assumed to impart considerable hydrophobicity to 5-FU. The purified and dried 5-FUDIPAL was further subjected to structural and physico-chemical characterization.

### 3.2. Characterization of 5-FUDIPAL

The two products 5-FUBHM and 5-FUDIPAL were characterized by FT-IR and  $^1\text{H}$ -NMR analysis. The FT-IR spectra of the products confirm the synthetic methodology, as depicted in Fig. 1. The peak shows the stretching of the  $-\text{OH}$  band at  $3330\text{ cm}^{-1}$  (peak a) and aliphatic  $-\text{C}-\text{H}$  by the methylenic group at  $2927\text{ cm}^{-1}$  (peak b). The peak at  $1670\text{ cm}^{-1}$  can be attributed to  $-\text{C}=\text{O}$  bond of 5-FU (peak c), and the peak at  $1060\text{ cm}^{-1}$  (peak d) may be assigned to  $-\text{C}-\text{F}$ -stretching vibrations of 5-FU aromatic ring. The  $\text{C}=\text{O}$  stretching vibration of the ester bond is shown at peak  $1724\text{ cm}^{-1}$ , specially formed in 5-FUDIPAL, which is absent in the initial spectra (peak e).

The  $^1\text{H}$  NMR spectrum of 5-FUBHM and 5-FUDIPAL (Fig. 2) clearly indicates that the peak at (4.6  $\delta$ ) is due to  $-\text{CH}_2-$  of the hydroxymethyl group. Peak b (2.1  $\delta$ ) shows the  $-\text{OH}$  stretching of the hydroxymethyl group. Peaks c and i (7.7  $\delta$ ) were due to the aromatic  $-\text{CH}$  proton of 5-FU. Further, peaks d, e, f and g (0.9–1.8  $\delta$ ) may be assigned to the methyl and methylenic groups of palmitic acid. Peak h (5.6–5.8  $\delta$ ) denotes the bridging methylenic group between 5-FU and palmitic acid.

DSC analysis of 5-FU and palmitic acid in comparison with 5-FUDIPAL confirms the formation of product and the removal of starting material (Fig. 4a). The melting point curves of 5-FU (melting point =  $282^\circ\text{C}$ ) and palmitic acid (melting point =  $63^\circ\text{C}$ ) were completely absent in the product. The 5-FUDIPAL showed a  $T_g$  (glass transition temperature) at  $98^\circ\text{C}$ .

### 3.3. Encapsulation of 5-FUDIPAL in polyester nanoparticles

The polyester nanoparticles were obtained with good yield and high purity. The double-emulsion solvent–evaporation technique generated  $\sim 90\%$  yield in all three polyester nanoparticulate systems (Table 1). Encapsulation efficiency calculations illustrated

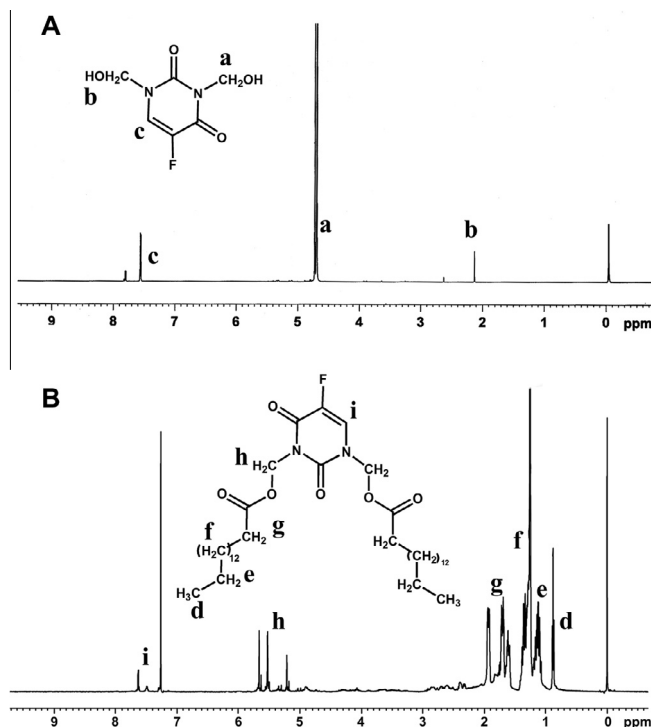


Fig. 2.  $^1\text{H}$ -NMR spectra of (A) 5-FUBHM and (B) 5-FUDIPAL.

>92% in all cases, which was profoundly better than earlier reports of 5-FU encapsulation. The extent of encapsulation followed the order  $\text{PCL} > \text{PLGA} > \text{PLA}$ , which is also the order of hydrophilicity of polymers. The higher encapsulation observed in PCL in comparison with PLGA and PLA may be attributed to the inherent structural hydrophobicity of the polymer.

### 3.4. Characterization of nanoparticles

Particle size analysis of the nanoparticles formed confirms the size range  $<150\text{ nm}$  for all the samples, as illustrated in Table 1. The nanoparticles formed were monodisperse in nature, with good homogeneity in distribution. All three samples showed an acceptable value of the polydispersity index, supporting the fact of uniform size distribution (Fig. S1, Table 1). The zeta potential is a parameter indicating the surface charge of the nanoparticles. The present authors observed a negative value of zeta potential, suggesting the stability of nanoparticles in the dispersion state (Table 1).

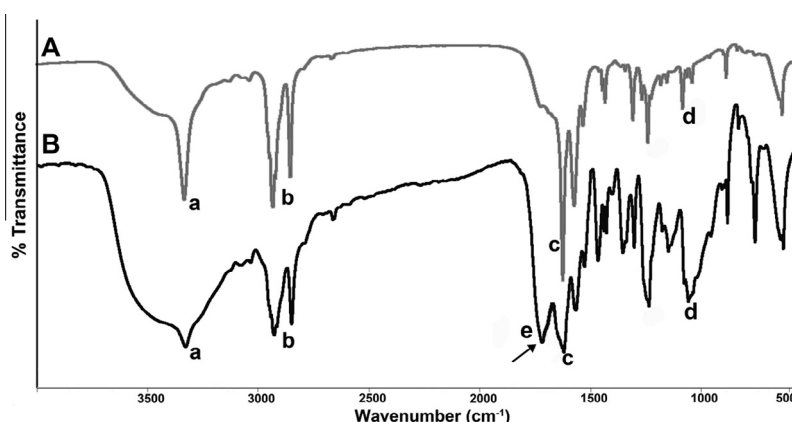


Fig. 1. FT-IR spectra of (A) 5-FUBHM and (B) 5-FUDIPAL.



**Table 1**

Characterization of 5-FUDIPAL entrapped polyester nanoparticles.

Sample (nanoparticle)	Encapsulation efficiency (%)	Yield (%)	Mean diameter (nm)	Poly dispersity index	Zeta potential (mV)
PLGA + 5-FUDIPAL	92.93 ± 0.39 <sup>a</sup>	95.2 ± 1.8 <sup>a</sup>	124.1 ± 4.3 <sup>a</sup>	0.159 ± 0.017 <sup>a</sup>	−17.7 ± 2.3 <sup>a</sup>
PLA + 5-FUDIPAL	90.41 ± 0.23 <sup>a</sup>	92.9 ± 2.1 <sup>a</sup>	127.7 ± 5.2 <sup>b</sup>	0.197 ± 0.008 <sup>a</sup>	−16.5 ± 1.4 <sup>a</sup>
PCL + 5-FUDIPAL	96.92 ± 0.28 <sup>a</sup>	96.3 ± 1.6 <sup>a</sup>	147.1 ± 3.5 <sup>a</sup>	0.169 ± 0.025 <sup>a</sup>	−8.6 ± 3.1 <sup>b</sup>

Values represents mean ± SD (n = 3).

<sup>a</sup> Value was found to be significant ( $p < 0.05$ ).<sup>b</sup> Value was found to be not significant ( $p \geq 0.05$ ).

Morphological analysis carried out by TEM shows the even distribution over the grid. The spherical nature of nanoparticles was well evident from TEM pictures (Fig. 3). The surface morphology of the nanoparticles was visualized by SEM analysis. The nanoparticles exhibited a smooth spherical surface and aggregation pattern, irrespective of the nature of the polymer (Fig. 3). The aggregation in SEM may be due to the lyophilized nanoparticles, which occur in the form of small clusters in dry state. While in TEM analysis the nanoparticles are well separated from each other. This can be attributed to the fact that they are readily dispersed in liquid state to distinct entities, which leads to minimum agglomeration.

DSC analysis was performed to assess the thermal stability of FUDIPAL encapsulated nanoparticles. DSC of the polyester nanoparticles with 5-FUDIPAL was compared with free polymer, and it was found that the peak of 5-FUDIPAL was missing in the curve (Fig. 4). This indicates that the drug is homogeneously dispersed inside the polymeric matrix. The thermal stability of the nanoparticles up to 200 °C was clearly observed in the DSC curves by the constant heat flow shown by nanoparticles as the temperature increased.

In order to monitor the amorphous nature of the nanoparticles and to study the nature of distribution of 5-FUDIPAL inside the polymeric matrix, XRPD analysis was carried out (Fig. 5). The XRPD curves of PLGA, PLA, PCL (b, c and d) show an absence of 2θ values of the reference curve of 5-FUDIPAL. This substantiates the fact of loss of the crystalline nature of the prodrug inside the polymeric nanoparticles and its even distribution [8].

### 3.5. Controlled release of 5-FUDIPAL from polyester nanoparticles

To assess the release pattern of 5-FUDIPAL from the polyester nanoparticles in vitro, kinetics studies were performed. Release studies clearly indicated the controlled release of 5-FUDIPAL from

PLGA, PCL and PLA. The release pattern observed in all the combinations follow the Peppas model [27] of drug release. The release pattern is given in Fig. 6. During the initial 60 min, all three systems showed a burst release pattern. PCL showed considerably slower release over the period of time (up to 900 min). The experiment was carried out up to 900 min because this was described as the gastrointestinal retention time in the literature [28]. PLA showed a higher amount of release in comparison with the other two nanoparticles during the initial 120 min. This is attributed to the polar nature of the polymer. Then, up to 300 min, PLGA showed a higher amount of 5-FUDIPAL release. From 300 to 900 min, PLA exhibited a higher amount of release. After 660 min, there was only a slight increase in the cumulative amount of 5-FUDIPAL released.

### 3.6. Significantly greater in vitro cytotoxicity exhibited by 5-FUDIPAL than 5-FU in blank form and in nano formulation

Cytotoxicity measurements were carried out by MTT assay in the HCT-116 cell line. To evaluate the pharmacological efficacy of 5-FUDIPAL and its nano formulation, MTT assay was found to be highly competent. The results indicated that the prodrug was more effective than free drug, and the modification increased the pharmacological potency (Fig. 7). After 24 h for 5 μM, 25 μM, 50 μM and 75 μM concentration, 5-FUDIPAL was showing higher inhibition than 5-FU. A similar trend was observed after 48 and 72 h for all experimental concentrations.

In order to monitor the competence of nano formulations of 5-FUDIPAL encapsulated nanoparticles, an MTT assay was done in the HCT-116 cell line. Cytotoxicity measurements on PLGA nanoparticles revealed that 5-FUDIPAL-encapsulated PLGA nanoparticles exhibited higher cytotoxicity than that of 5-FUDIPAL over a range of experimental concentrations against the tumour cell line. In 24 h, PLGA nanoparticles showed slightly higher activity than

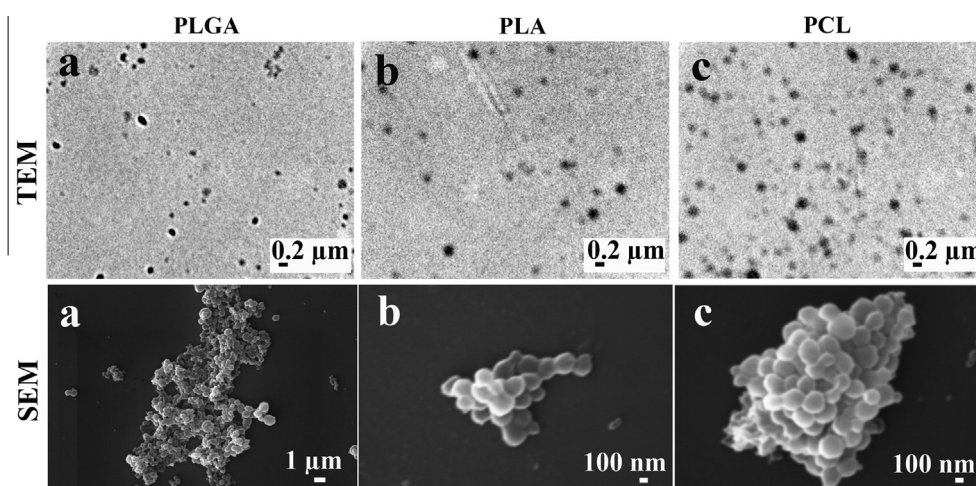


**Fig. 3.** Nanoparticle size and morphological characterization. SEM image of 5-FUDIPAL encapsulated nanoparticles: (a) PLGA; (b) PLA; (c) PCL. TEM image of 5-FUDIPAL encapsulated nanoparticles: (a) PLGA; (b) PLA; (c) PCL.

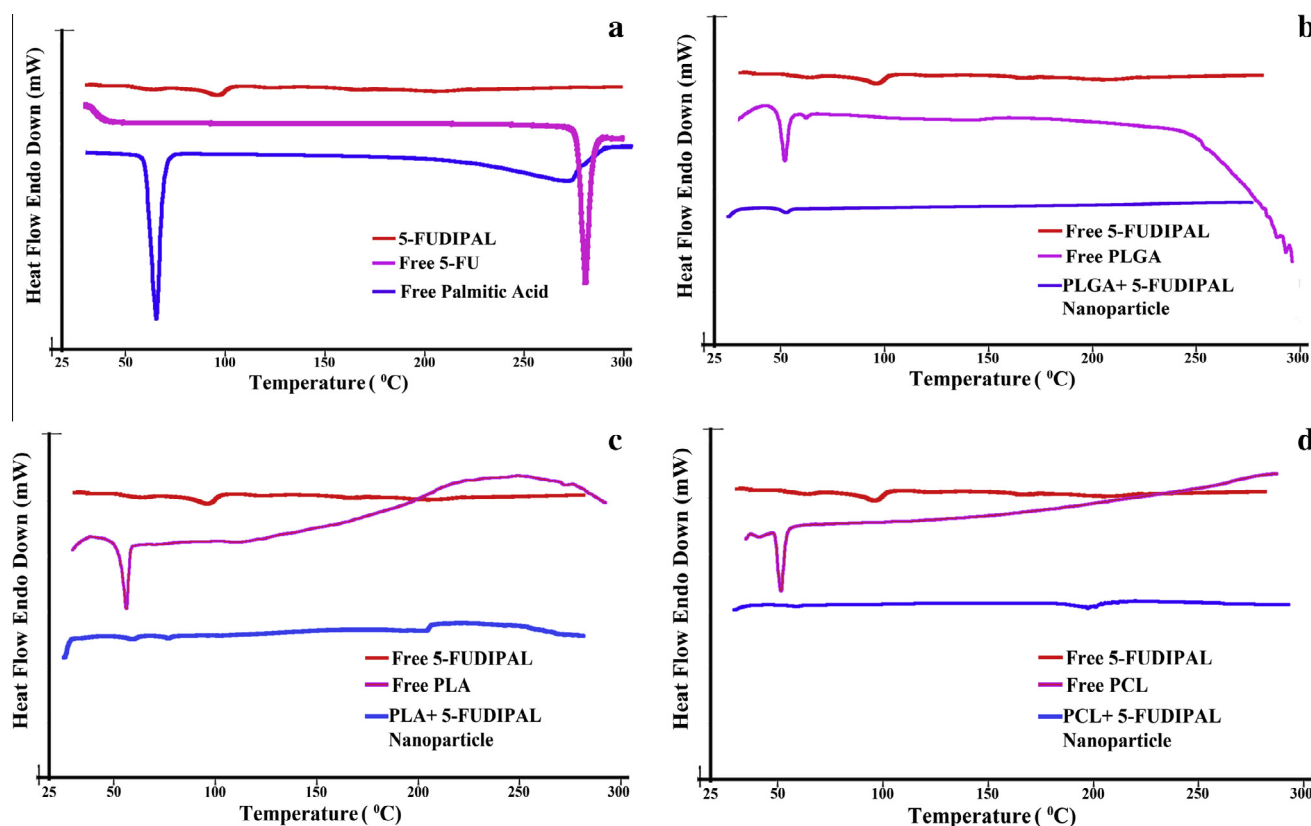


Fig. 4. DSC thermograms of (a) 5-FUDIPAL compared with 5-FU and palmitic acid, and (b–d) 5-FUDIPAL encapsulated PLGA, PLA and PCL nanoparticles, respectively.

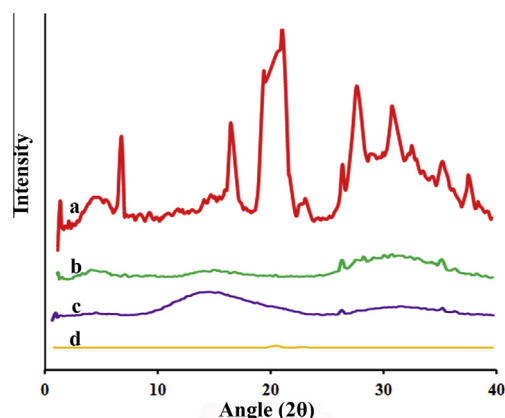


Fig. 5. XRPD pattern of (a) blank 5-FUDIPAL (b) 5-FUDIPAL entrapped PLGA nanoparticles, (c) 5-FUDIPAL entrapped PLA nanoparticles, and (d) 5-FUDIPAL entrapped PCL nanoparticles.

the free 5-FUDIPAL. But the activity was found to be significantly increased after 48 and 72 h (Fig. 7). After 48 h, a 50  $\mu$ M concentration of PLGA with 5-FUDIPAL showed an inhibition of 59.4%, whereas 5-FUDIPAL alone showed 51.7%; 75  $\mu$ M of nanoformulation had an inhibition of 63%, while free 5-FUDIPAL possessed only 54.9% inhibition. After 72 h, 50  $\mu$ M and 75  $\mu$ M of PLGA with 5-FUDIPAL demonstrated an inhibition of 86.0% and 87.8%, respectively, whereas free 5-FUDIPAL had 80.3% and 84.6% inhibition. At all three times (24, 48 and 72 h), 5-FUDIPAL and 5-FUDIPAL-entrapped nanoparticles exhibited better inhibition than free 5-FU. A comparison of  $ic_{50}$  values was calculated for the MTT data (Fig. 7) from the dose–response curve, as illustrated in Table 2.

PCL and PLA nanoparticles also displayed significant cytotoxicity in comparison with free 5-FUDIPAL (Fig. 8). After 24 h, the PLA

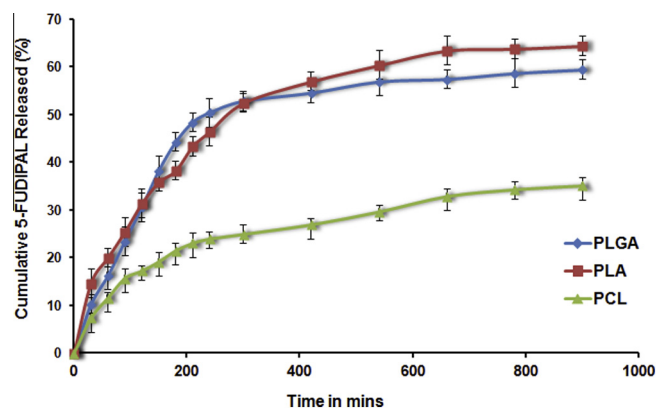
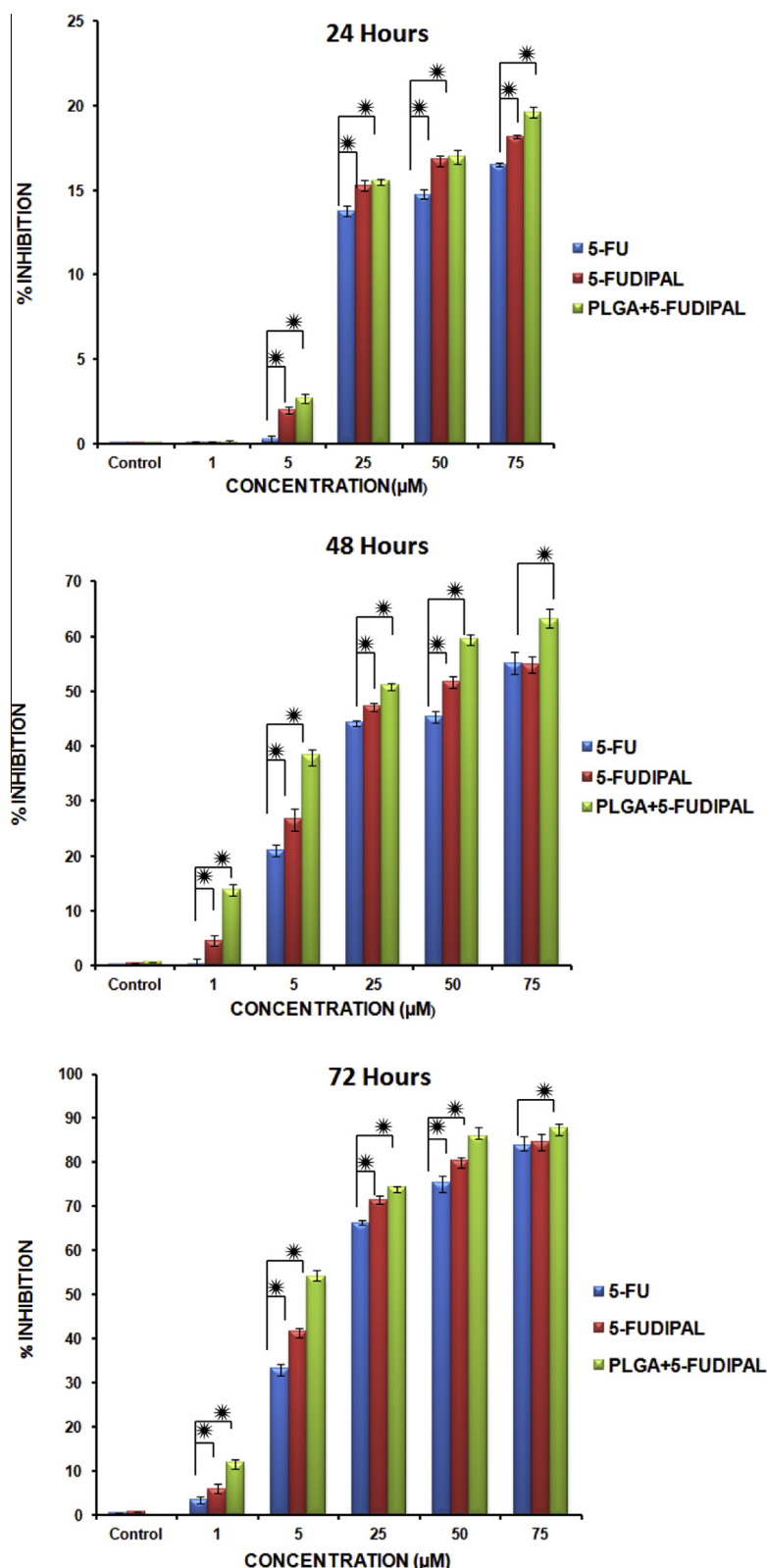


Fig. 6. In vitro drug release profile of 5-FUDIPAL from different nanoparticulate systems. Data shown are mean value  $\pm$  standard deviation (SD) ( $n = 3$ ,  $*p < 0.05$ ).

nanoparticles showed higher activity than that of 5-FUDIPAL in various concentrations, including 5  $\mu$ M, 10  $\mu$ M, 50  $\mu$ M and 100  $\mu$ M, while 5-FUDIPAL-entrapped PCL nanoparticles featured better inhibition in different concentrations, including 1  $\mu$ M, 50  $\mu$ M and 100  $\mu$ M. After 48 h, PLA nanoparticles revealed better cytotoxicity in 1  $\mu$ M, 10  $\mu$ M, 50  $\mu$ M and 100  $\mu$ M concentrations. PCL nanoparticles exhibited higher cytotoxicity in all the experimental concentrations.

#### 4. Discussion

Smart biomaterials such as nanoparticles were able to deliver encapsulated anti-cancer agents to the tumour site with a high degree of specificity and selectivity [29,30]. The prodrug-based



**Fig. 7.** MTT assay of 5-FUDIPAL encapsulated PLGA nanoparticles. Cytotoxicity to HCT-116 cells induced by blank 5-FU (1–75 μM), blank 5-FUDIPAL (1–75 μM) and 5-FUDIPAL encapsulated in PLGA nanoparticles (1–75 μM) on incubation for 24 h, 48 h and 72 h. Data shown are mean value  $\pm$  SD ( $n = 3$ ,  $*p < 0.05$ ).

approach of 5-FU, such as capecitabine [31] and ftorafur [32], was done earlier to prevent the degradation of 5-FU by the action of DPD enzyme. But the inherent hydrophilic nature of the 5-FU remains the same, and <80% encapsulation efficiency was observed in nanoform [33]. Increasing the amount of encapsulation of

antineoplastic agents per nanoparticle will lead to an improved therapeutic window of the formulation. The present authors' study describes the preparation and evaluation of a prodrug of 5-FU with higher hydrophobicity and its efficacy in various nanoformulations consisting of USFDA approved polyesters (PLGA, PLA and PCL) for

**Table 2** $i_{C50}$  values comparison of 5-FU, 5-FUDIPAL and 5-FUDIPAL + PLGA.

Incubation time (h)	$i_{C50}$ values ( $\mu$ M)		
	5-FU	5-FUDIPAL	5-FUDIPAL + PLGA
48	67.83 <sup>a</sup>	35.11 <sup>a</sup>	23.43 <sup>a</sup>
72	15.25 <sup>a</sup>	11.61 <sup>a</sup>	4.65 <sup>a</sup>

Data represents mean  $\pm$  SD ( $n = 3$ ).<sup>a</sup> Value was found to be significant ( $p < 0.05$ ).

drug delivery systems. The main objective of the study was to modify the conventional CDDS of USFDA-approved polymers with a prodrug of 5FU with increased encapsulation and a higher degree of cytotoxicity to the tumour.

In order to synthesize the prodrug, we have used a biocompatible lipid moiety, namely palmitic acid. The conjugation was brought about by the generated intermediate 5-FUBHM. The facile synthesis and higher degree of purification ensured the complete elimination of formaldehyde in the first step of the methodology (Scheme 1). This was an important step, because of the inherent toxicity exhibited by the formaldehyde [34], which might alter the action of the prodrug. Further the generation of two hydroxymethyl groups at the N-1 and N-3 positions of 5-FU enabled the conjugation of palmitic acid through an ester bond. Spectral (FT-IR, <sup>1</sup>H-NMR) and thermal (DSC) characterization ensured the complete synthesis of 5-FUDIPAL devoid of impurities. The solubility shift in the synthesized 5-FUDIPAL from the polar solvent (water) to non-polar solvent (DCM) opened up a new avenue for the encapsulation in nano formulation with high efficacy. As 5-FU is soluble in water, a low amount (<80%) of encapsulation in polymers such as PLGA, PLA and PCL was observed [8–10] by virtue of its

hydrophobicity and loss of drug molecule in the process of washing and recovery of nanoparticles. The present strategy provided a platform to prepare the nanoparticles with a higher amount of encapsulation.

The preparation of nanoparticles within the size range 120–150 nm and with a surface charge of  $-18$  mV to  $-8$  mV was expected to be readily taken up by the tumour microenvironment by the enhanced permeability and retention effect [27]. Further, the anionic charge of the nanoparticles facilitates efficient evasion from renal elimination [35,36]. These factors facilitate the delivery of the encapsulated antineoplastic agent by means of passive targeting from the polyester nanoparticles [37]. SEM and TEM analysis substantiated the nano size and spherical nature of nanoparticles. DSC and XRPD analysis confirmed the thermal stability, amorphous nature and uniform distribution of 5-FUDIPAL inside the polymeric nanoparticles. Further, the in vitro release profile demonstrated the sustained release of 5-FUDIPAL from the nanoparticles. Based on the above observations, we propose the plausible encapsulation and distribution mechanism of 5-FUDIPAL in polyester nanoparticles, as depicted in Scheme 2. The conjugated palmitic acid tails were assumed to elevate the non-covalent interaction (hydrophobic interaction between fatty acid and polyesters) between the prodrug and the polymer. This type of attraction results in a high amount of drug loading and controlled release phenomenon.

The biological evaluation of prodrug encapsulated nanoparticles by cytotoxicity measurements displayed higher cytotoxicity in the majority of concentrations. Blank 5-FUDIPAL itself displayed more cytotoxicity than 5-FU at all experimental times. The nano formulations of 5-FUDIPAL at different concentrations were also highly potent in inducing cytotoxicity at all experimental times (Fig. 7 and Table 2). A comparison of  $i_{C50}$  values shows that the prodrug

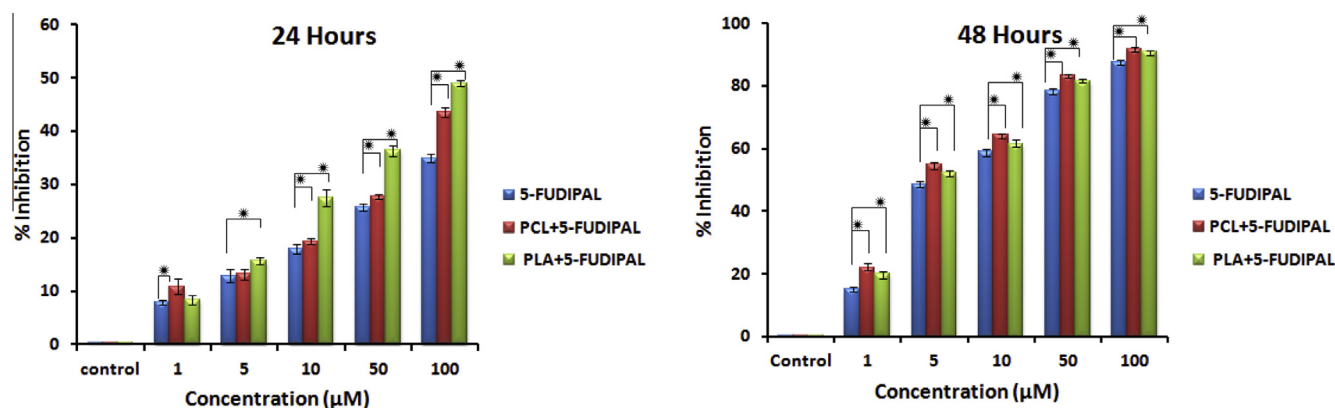
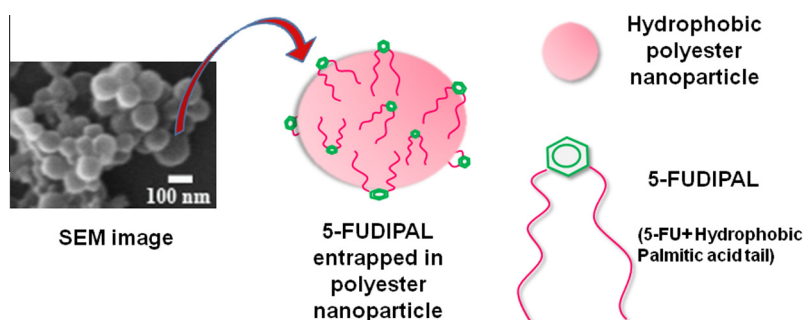


**Fig. 8.** MTT assay of 5-FUDIPAL encapsulated PLA and PCL nanoparticles. Cytotoxicity to HCT-116 cells induced by blank 5-FUDIPAL (1–100  $\mu$ M), 5-FUDIPAL encapsulated in PCL nanoparticles (1–100  $\mu$ M) and PLA nanoparticles (1–100  $\mu$ M) on incubation for 24 h and 48 h. Data shown are mean value  $\pm$  SD ( $n = 3$ , \* $p < 0.05$ ).



**Scheme 2.** Plausible mechanism of loading of 5-FUDIPAL in polyester-based nanoparticles.



had values almost two times lower than the free 5-FU after 48 h, whereas the nanoformulation (PLGA nanoparticles with 5-FUDIPAL) had an  $ic_{50}$  value three times lower than the free 5-FU after 48 h. A similar trend also continued for the nanoformulation after 72 h (Table 2). Other nano forms of 5-FUDIPAL such as PLA and PCL nanoparticles were also more efficient in inducing cytotoxicity than the naïve prodrug, as observed from the MTT assay (Fig. 8).

The induction of cytotoxicity by the nanoformulation at a much lower concentration than the free drug was highly promising for a good CDDS. Even though more biological studies are inevitable, we propose the cleavage of the ester bond of the prodrug (by esterase enzyme), which gives 5-FUBHM and 5-FU afterwards in a stepwise manner. The cleavage of the ester bond in *in vivo* conditions was reported earlier [38], and therapeutic action for 5-FUBHM was also mentioned [39]. These points substantiate the present hypothesis, and 5-FUDIPAL is presented as potent candidate for DDS in hydrophobic polyester-based nanoparticles.

## 5. Conclusions

The synthesis of a lipid drug conjugate revealed that 5-FU can be conjugated without losing its cytotoxicity to the lipid. This was a structural-based approach to facilitate enhanced loading into the nanoparticulate system. The formation of nanoparticles with higher encapsulation efficiency is an added advantage to this strategy. Further MTT assay revealed that the modified lipid drug conjugate will be a suitable candidate for the encapsulation of 5-FU in hydrophobic polymeric nanoparticles in the area of cancer chemotherapy. More biological studies are essential for understanding the mechanism by which the 5-FUDIPAL induces cell death in both naïve and nano formulation, thereby bringing cytotoxicity to the tumour.

## Acknowledgments

The authors are grateful to Ms. Rintu Varghese of the Rajiv Gandhi Centre for Biotechnology (RGCB) for TEM analysis, the National Institute for Interdisciplinary Science and Technology (NIIST) Trivandrum for NMR and SEM analysis, STIC (Cochin University of Science and Technology, Cochin, Kerala) for XRPD analysis, the Department of Biotechnology, New Delhi, for providing the financial assistance for the research work and the Council of Scientific and Industrial Research (CSIR), New Delhi, for the Junior Research Fellowship to N. Ashwanikumar.

## Appendix A. Figures with essential color discrimination

Certain figures in this article, particularly Figs. 4–8 and Scheme 2 are difficult to interpret in black and white. The full color images can be found in the on-line version, at <http://dx.doi.org/10.1016/j.actbio.2014.07.032>.

## Appendix B. Supplementary data

Supplementary data associated with this article can be found, in the online version, at <http://dx.doi.org/10.1016/j.actbio.2014.07.032>.

## References

- [1] Kwon S, Singh RK, Kim TH, Patel KD, Kim JJ, Chrzanowski W, et al. Luminescent mesoporous nanoreservoirs for the effective loading and intracellular delivery of therapeutic drugs. *Acta Biomater* 2014;10:1431–42.
- [2] Yoo JW, Irvine DJ, Discher DE, Mitragotri S. Bio-inspired, bioengineered and biomimetic drug delivery carriers. *Nat Rev Drug Discov* 2011;10:521–35.
- [3] Spataro G, Malecaze F, Turrin CO, Soler V, Duhayon C, Elena PP, et al. Designing dendrimers for ocular drug delivery. *Eur J Med Chem* 2010;45:326–34.
- [4] Brigger I, Dubernet C, Couvreur P. Nanoparticles in cancer therapy and diagnosis. *Adv Drug Deliv Rev* 2012;64(Suppl.):24–36.
- [5] Saxena A, Mozumdar S, Johri AK. Ultra-low sized cross-linked polyvinylpyrrolidone nanoparticles as non-viral vectors for *in vivo* gene delivery. *Biomaterials* 2006;27:5596–602.
- [6] Meng H, Liong M, Xia T, Li Z, Ji Z, Zink JJ, et al. Engineered design of mesoporous silica nanoparticles to deliver doxorubicin and P-glycoprotein siRNA to overcome drug resistance in a cancer cell line. *ACS Nano* 2010;4:4539–50.
- [7] Agasti SS, Chomposor A, You CC, Ghosh P, Kim CK, Rotello VM. Photoregulated release of caged anticancer drugs from gold nanoparticles. *J Am Chem Soc* 2009;131:5728–9.
- [8] Nair KL, Jagadeeshan S, Nair SA, Kumar GSV. Biological evaluation of 5-fluorouracil nanoparticles for cancer chemotherapy and its dependence on the carrier, PLGA. *Int J Nanomedicine* 2011;6:1685–97.
- [9] Blanco M, Sastre R, Teijon C, Olmo R, Teijon JM. 5-Fluorouracil-loaded microspheres prepared by spray-drying poly (D, L-lactide) and poly (lactide-co-glycolide) polymers: characterization and drug release. *J Microencapsul* 2005;22:671–82.
- [10] Sastre RL, Blanco MD, Teijon C, Olmo R, Teijon JM. Preparation and characterization of 5-fluorouracil-loaded poly (ε-caprolactone) microspheres for drug administration. *Drug Dev Res* 2004;63:41–53.
- [11] Parveen S, Misra R, Sahoo SK. Nanoparticles: a boon to drug delivery, therapeutics, diagnostics and imaging. *Nanomedicine* 2012;8:147–66.
- [12] Acharya S, Sahoo SK. PLGA nanoparticles containing various anticancer agents and tumour delivery by EPR effect. *Adv Drug Deliv Rev* 2011;63:170–83.
- [13] Danhier F, Ansorena E, Silva JM, Coco R, Le Breton A, Preat V. PLGA-based nanoparticles: an overview of biomedical applications. *J Control Release* 2012;161:505–22.
- [14] Longley DB, Harkin DP, Johnston PG. 5-Fluorouracil: mechanisms of action and clinical strategies. *Nat Rev Cancer* 2003;3:330–8.
- [15] Di Paolo A, Danesi R, Falcone A, Cionini L, Vannozzi F, Masi G, et al. Relationship between 5-fluorouracil disposition, toxicity and dihydropyrimidine dehydrogenase activity in cancer patients. *Ann Oncol* 2001;12:1301–6.
- [16] van Kuilenburg AB. Dihydropyrimidine dehydrogenase and the efficacy and toxicity of 5-fluorouracil. *Eur J Cancer* 2004;40:939–50.
- [17] Fata F, Ron IG, Kemeny N, O'Reilly E, Klimstra D, Kelsen DP. 5-Fluorouracil-induced small bowel toxicity in patients with colorectal carcinoma. *Cancer* 1999;86:1129–34.
- [18] Contino C, Maurizis JC, Pucci B. Synthesis and preliminary biological assessments of a new class of amphiphilic telomers bearing 5-fluorouracil moieties. *Macromol Chem Phys* 1999;200:1351–5.
- [19] Nichifor M, Schacht EH, Seymour LW. Polymeric prodrugs of 5-fluorouracil. *J Control Release* 1997;48:165–78.
- [20] Ashwanikumar N, Kumar NA, Nair SA, Kumar GSV. Methacrylic-based nanogels for the pH-sensitive delivery of 5-Fluorouracil in the colon. *Int J Nanomed* 2012;7:5769–79.
- [21] Mahato R, Tai W, Cheng K. Prodrugs for improving tumor targetability and efficiency. *Adv Drug Deliv Rev* 2011;63:659–70.
- [22] Liu Z, Rimmer S. Synthesis and release of 5-fluorouracil from poly (N-vinylpyrrolidone) bearing 5-fluorouracil derivatives. *J Control Release* 2002;81:91–9.
- [23] Liu Z, Fullwood N, Rimmer S. Synthesis of allyloxycarbonyloxymethyl-5-fluorouracil and copolymerizations with N-vinylpyrrolidone. *J Mater Chem* 2000;10:1771–5.
- [24] Soman A, Qiu Y, Li QC. HPLC-UV method development and validation for the determination of low level formaldehyde in a drug substance. *J Chromatogr Sci* 2008;46:461–5.
- [25] Lu XY, Zhang Y, Wang L. Preparation and *in vitro* drug-release behavior of 5-fluorouracil-loaded poly (hydroxybutyrate-co-hydroxyhexanoate) nanoparticles and microparticles. *J Appl Polym Sci* 2010;116:2944–50.
- [26] Abdelwahed W, Degobert G, Stainmesse S, Fessi H. Freeze-drying of nanoparticles: formulation, process and storage considerations. *Adv Drug Deliv Rev* 2006;58:1688–713.
- [27] Owens III DE, Peppas NA. Opsonization, biodistribution, and pharmacokinetics of polymeric nanoparticles. *Int J Pharm* 2006;307:93–102.
- [28] Yang L, Chu JS, Fix JA. Colon-specific drug delivery: new approaches and *in vitro/in vivo* evaluation. *Int J Pharm* 2002;235:1–15.
- [29] Fang JY, Al-Suwayeh SA. Nanoparticles as delivery carriers for anticancer prodrugs. *Expert Opin Drug Deliv* 2012;9:657–69.
- [30] Li MH, Choi SK, Thomas TP, Desai A, Lee KH, Kotlyar A, et al. Dendrimer-based multivalent methotrexates as dual acting nanoconjugates for cancer cell targeting. *Eur J Med Chem* 2012;47:560–72.
- [31] Schuller J, Cassidy J, Dumont E, Roos B, Durston S, Banken L, et al. Preferential activation of capecitabine in tumor following oral administration to colorectal cancer patients. *Cancer Chemother Pharmacol* 2000;45:291–7.
- [32] Adjei AA. A review of the pharmacology and clinical activity of new chemotherapy agents for the treatment of colorectal cancer. *Br J Clin Pharmacol* 1999;48:265–77.
- [33] Wei K, Peng X, Zou F. Folate-decorated PEG–PLGA nanoparticles with silica shells for capecitabine controlled and targeted delivery. *Int J Pharm* 2014;464:225–33.
- [34] Duong A, Steinmaus C, McHale CM, Vaughan CP, Zhang L. Reproductive and developmental toxicity of formaldehyde: a systematic review. *Mutat Res* 2011;728:118–38.

- [35] Malam Y, Loizidou M, Seifalian AM. Liposomes and nanoparticles: nanosized vehicles for drug delivery in cancer. *Trends Pharmacol Sci* 2009;30:592–9.
- [36] Gullotti E, Yeo Y. Extracellularly activated nanocarriers: a new paradigm of tumor targeted drug delivery. *Mol Pharm* 2009;6:1041–51.
- [37] Danhier F, Feron O, Preat V. To exploit the tumor microenvironment: passive and active tumor targeting of nanocarriers for anti-cancer drug delivery. *J Control Release* 2010;148:135–46.
- [38] Sagnella SM, Gong X, Moghaddam MJ, Conn CE, Kimpton K, Waddington LJ, et al. Nanostructured nanoparticles of self-assembled lipid pro-drugs as a route to improved chemotherapeutic agents. *Nanoscale* 2011;3:919–24.
- [39] McCarron P, Hall M. Incorporation of novel 1-alkylcarbonyloxymethyl prodrugs of 5-fluorouracil into poly (lactide-co-glycolide) nanoparticles. *Int J Pharm* 2008;348:115–24.